The calibration of carbon nanotube based bionanosensors

S. Adhikari[a] and R. Chowdhury[a]
Multidisciplinary Nanotechnology Centre, Swansea University, Singleton Park, Swansea SA2 8PP, United Kingdom

(Received 25 March 2010; accepted 28 April 2010; published online 28 June 2010)

We derive the calibration constants necessary for using single-walled carbon nanotubes (CNTs) as nanoscale mass sensors. The CNT resonators are assumed to be either in cantilevered or in bridged configurations. Two cases, namely, when the added mass can be considered as a point mass and when the added mass is distributed over a larger area is considered. Closed-form transcendental equations have been derived for the frequency shift due to the added mass. Using the energy principles, generalized nondimensional calibration constants have been derived for an explicit relationship between the added mass and the frequency shift. A molecular mechanics model based on the universal force field potential is used to validate the new results presented. The results indicate that the distributed nature of the mass to be detected has considerable effect on the performance of the sensor. © *2010 American Institute of Physics*. [doi:10.1063/1.3435316]

I. INTRODUCTION

Carbon nanotubes (CNTs) have received significant attention over the past decade as a new class of nanomaterials.[1] CNTs are molecular scale tubes of graphitic carbon that possess exceptional structural/mechanical properties, as well as electronic, thermal,[1] and optical characteristics.[1] These lead to a variety of applications using CNTs in storage devices,[2–4] nanoelectronics, scanning probes,[5,6] nanoelectromechanical systems[7] to mention a few. Advances in materials synthesis have enabled the use of CNTs to the development of electrochemical sensing system,[8–11] nanosensors,[12–15] and nanoactuators.[16]

Nanoscale sensors[12–14,17–19] play crucial roles in environmental monitoring (e.g., detection of gas),[20] chemical process control,[21] and biomedical applications.[22–27] The use of a CNT to make the lightest inertial balance is essentially to make a ultrasensitive nanoscale mass spectrometer,[24,25] electroanalytical nanotube devices,[26,28] and electromechanical actuators for artificial muscles.[29] Nanobiosensors[30] are being developed on the fact that biological fragments can be immobilized either in the hollow cavity or on the surface of CNTs.[22,23] Building and designing such nanosensors that is able to make measurements of external deposited agents[29,31–33] with ultrahigh resolution[14,34] is one of the main goals in the field of nanomechanics and is the topic of this paper.

Resonance based sensors[12–14,17–19,35] offer significant potential of achieving the high-fidelity requirement of many sensing applications. The principle of mass detection using resonators is based on the fact that the resonant frequency is sensitive to the resonator mass. The resonator mass includes the self-mass of the resonator and the attached mass. The change in the attached mass on the resonator causes a shift to the resonant frequency. The key issue of mass detection is in quantifying the change in the resonant frequency due to the added mass. Majority of the existing works assume that the added mass is a "point mass," that is, the physical dimension of the added mass is very small compared to the dimension of resonator (CNT in this case). This assumption may not be always true, especially for biosensors as many biological objects such as DNA, proteins can have relatively larger dimensions. In this paper the distributed nature of the added mass is taken into account by assuming uniform mass distribution along the length of the CNT. The CNTs are assumed to be either in cantilevered or in bridged configurations. We derive the calibration constants necessary for using single-walled CNTs (SWCNTs) as a nanomechanical resonators in nanosized mass sensors. Two cases, namely, when the added mass can be considered as a point mass and when the added mass is distributed over a larger area is considered. Closed-form transcendental equations have been derived for the frequency shift due to the added mass in Sec. II. In Sec. III, using the energy principles, general expressions of the calibration constants have been derived. These calibration constants are calculated in Sec. IV for different cases. A molecular mechanics model based on the universal force field (UFF) potential[36] is used in Sec. V to benchmark the new results derived in the paper. The results obtained using the calibration constants are discussed in Sec. VI.

II. DYNAMICAL EQUATIONS OF MASS LOADED CNTS

A. Cantilevered CNT

For relatively long CNTs, atomistic simulation based approaches can be prohibitively expensive. Moreover, such an approach normally do not result any analytical relationship between the added mass and an observable quantities which can be exploited in a sensor design. This problem can be addressed if a continuum model based approach is adopted.[37–41] We use a rod model with Euler–Bernoulli beam bending theory.[42] In a previous study,[17] the static deflection of CNTs is used to obtain the sensor equations. In the present study dynamical equations are used. This is expected to result in more accurate sensing capability as the inertial prop-

[a]Electronic addresses: s.adhikari@swansea.ac.uk and r.chowdhury@swansea.ac.uk.

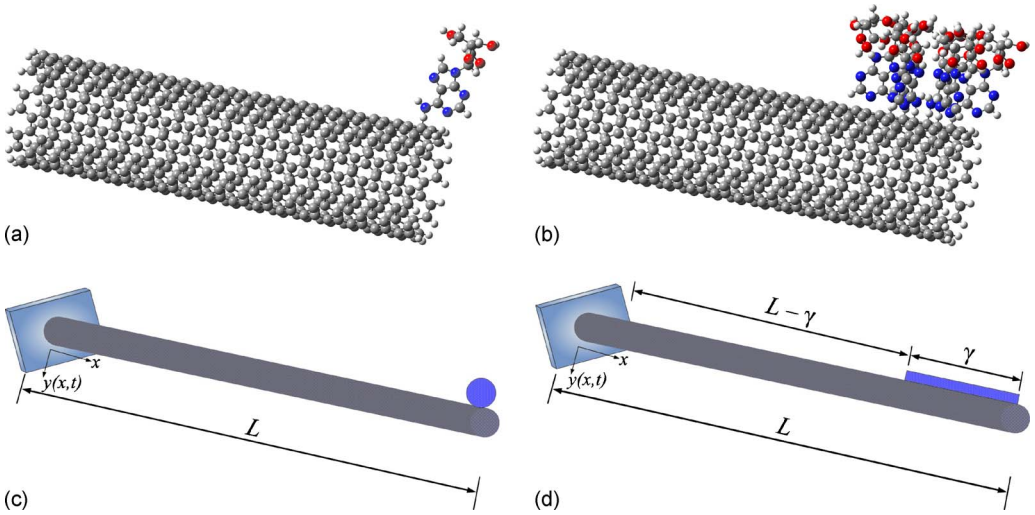

FIG. 1. (Color online) Cantilevered nanotube resonator with attached masses. Here, deoxythymidine is used as an example. (a) Original configuration with a point mass at the tip; (b) original configuration with distributed masses; (c) mathematical idealization with a point mass at the tip; and (d) mathematical idealization with distributed masses.

erties of the CNTs are taken into account in a more rigorous manner. The equation of motion of free-vibration can be expressed as

$$EI\frac{\partial^4 y(x,t)}{\partial x^4}+\rho A\frac{\partial^2 y(x,t)}{\partial t^2}=0, \tag{1}$$

where x is the coordinate along the length of the CNT, t is the time, $y(x,t)$ is the transverse displacement of the CNT, E is the Young's modulus, I is the second-moment of the cross-sectional area A, and ρ is the density of the material. Suppose the length of the SWCNT is L. For the cantilevered CNT, the resonance frequencies can be obtained from

$$f_j=\frac{\lambda_j^2}{2\pi}\sqrt{\frac{EI}{\rho AL^4}}, \tag{2}$$

where λ_j can be obtained by[43] solving the following transcendental equation:

$$\cos\lambda\cosh\lambda+1=0. \tag{3}$$

The vibration mode shape can be expressed as

$$Y_j(\xi)=(\cosh\lambda_j\xi-\cos\lambda_j\xi)-\left(\frac{\sinh\lambda_j-\sin\lambda_j}{\cosh\lambda_j+\cos\lambda_j}\right)\times(\sinh\lambda_j\xi-\sin\lambda_j\xi), \tag{4}$$

where

$$\xi=\frac{x}{L}, \tag{5}$$

is the normalized coordinate along the length of the CNT. For sensing applications we are interested in the first mode of vibration for which $\lambda_1=1.8751$.

Suppose there is an attached nano/bio-object of mass M at the end of the cantilevered resonator in Fig. 1(a). The boundary conditions with an additional mass of M at $x=L$ can be expressed as

$$y(0,t)=0,\quad y'(0,t)=0,\quad y''(L,t)=0,\quad \text{and}\quad EIy'''(L,t)-M\ddot{y}(L,t)=0. \tag{6}$$

Here $(\bullet)'$ denotes derivative with respective to x and $(\dot{\bullet})$ denotes derivative with respective to t. Assuming harmonic solution $y(x,t)=Y(x)e^{i\omega t}$ and using the boundary conditions, it can be shown that the resonance frequencies are still obtained from Eq. (2) but λ_j should be obtained by solving

$$(\cos\lambda\sinh\lambda-\sin\lambda\cosh\lambda)\Delta M\lambda+(\cos\lambda\cosh\lambda+1)=0. \tag{7}$$

Here

$$\Delta M=\frac{M}{\rho AL}, \tag{8}$$

is the ratio of the added mass and the mass of the CNT. If the added mass is zero, then one can see that Eq. (8) reduces to Eq. (3).

B. Bridged CNT

For the bridged CNT shown in Fig. 2, the frequency is given by Eq. (2) where λ_j should be obtained[43] by solving

$$\cos\lambda\cosh\lambda-1=0 \tag{9}$$

The vibration mode shape can be expressed as

$$Y_j(\xi)=(\cosh\lambda_j\xi-\cos\lambda_j\xi)-\left(\frac{\cosh\lambda_j-\cos\lambda_j}{\sinh\lambda_j-\sin\lambda_j}\right)\times(\sinh\lambda_j\xi-\sin\lambda_j\xi). \tag{10}$$

For the first mode of vibration we have $\lambda_1=4.7300$.

Suppose there is an attached nano/bio-object of mass M at a distance θL $(0\le\theta\le1)$ from the left-hand side of the bridged resonator. In Fig. 2(a) this is shown for $\theta=1/2$, that is when the attached mass is at the middle of the SWCNT.

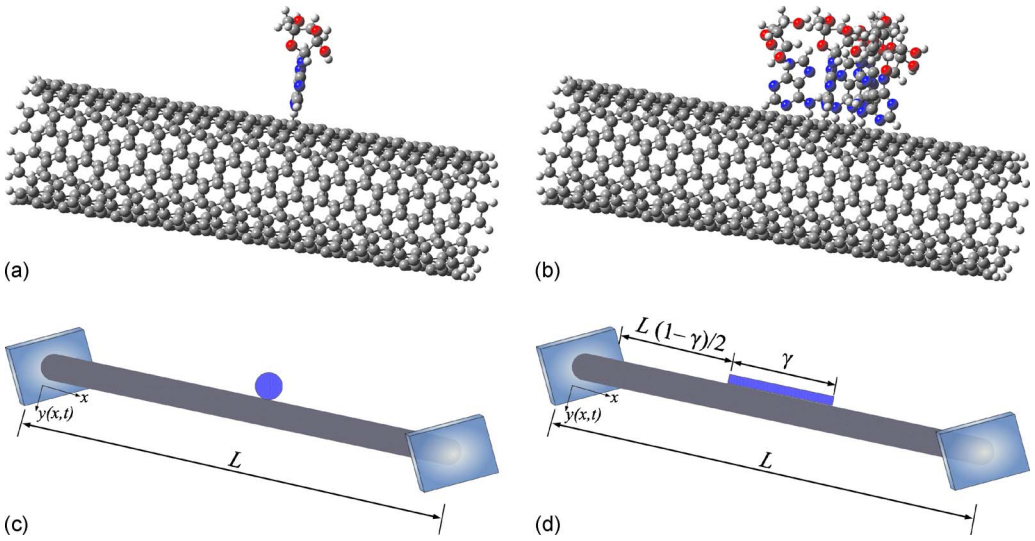

FIG. 2. (Color online) Bridged nanotube resonator with attached masses. Like the cantilevered case, deoxythymidine is used as an example. (a) Original configuration with a point mass at the center; (b) original configuration with distributed masses; (c) mathematical idealization with a point mass at the center; (d) mathematical idealization with distributed masses.

Denoting the deflection as $y_1(x,t)$ in the left side of the mass and $y_2(x,t)$ as the right side of the mass, the boundary conditions can be expressed as

$$y_2(0,t)=0, y_1'(0,t)=0, y_2(L,t)=0, y_2'(L,t)=0,$$

$$y_1(\theta L,t)=y_2(\theta L,t),$$

$$\begin{aligned} y_1'(\theta L,t) &= y_2'(\theta L,t), y_1''(\theta L,t) \\ &= y_2''(\theta L,t) \quad \text{and} \quad EIy_1'''(\theta L,t)-M\ddot{y}_1(\theta L,t) \\ &= EIy_2'''(\theta L,t). \end{aligned} \tag{11}$$

Using these it can be shown that the resonance frequencies are given by Eq. (2) where λ_j should be obtained by solving the following transcendental equation:

$$\begin{aligned} &(-s_{\lambda\theta}s_\lambda sh_{\lambda\theta}ch_\lambda - sh_{\lambda\theta}s_\lambda ch_{\lambda\theta}sh_\lambda - c_\lambda sh_\lambda c_{\lambda\theta}^2 \\ &\quad + s_{\lambda\theta}c_\lambda ch_{\lambda\theta}ch_\lambda + s_\lambda c_{\lambda\theta}sh_{\lambda\theta}sh_\lambda - s_{\lambda\theta}c_\lambda sh_{\lambda\theta}sh_\lambda \\ &\quad + c_{\lambda\theta}sh_{\lambda\theta} + s_{\lambda\theta}s_\lambda ch_{\lambda\theta}sh_\lambda + s_\lambda ch_\lambda ch_{\lambda\theta}^2 - s_{\lambda\theta}s_\lambda c_{\lambda\theta}sh_\lambda \\ &\quad - sh_{\lambda\theta}c_\lambda c_{\lambda\theta}ch_\lambda - s_{\lambda\theta}ch_{\lambda\theta} + c_\lambda c_{\lambda\theta}ch_{\lambda\theta}sh_\lambda \\ &\quad - ch_{\lambda\theta}c_{\lambda\theta}s_\lambda ch_\lambda)\lambda^2\Delta M + (s_{\lambda\theta}s_\lambda sh_{\lambda\theta}sh_\lambda - ch_{\lambda\theta}^2 s_\lambda sh_\lambda \\ &\quad + 1 + c_{\lambda\theta}^2 s_\lambda sh_\lambda - c_\lambda ch_\lambda - s_{\lambda\theta}s_\lambda ch_{\lambda\theta}ch_\lambda + c_{\lambda\theta}ch_{\lambda\theta} \\ &\quad - c_{\lambda\theta}c_\lambda ch_{\lambda\theta}ch_\lambda + ch_{\lambda\theta}s_\lambda sh_{\lambda\theta}ch_\lambda - s_{\lambda\theta}c_{\lambda\theta}c_\lambda sh_\lambda \\ &\quad + c_{\lambda\theta}c_\lambda sh_{\lambda\theta}sh_\lambda)\lambda - s_\lambda ch_\lambda ch_{\lambda\theta}^2 + s_\lambda ch_\lambda \\ &\quad + sh_{\lambda\theta}s_\lambda ch_{\lambda\theta}sh_\lambda - c_\lambda sh_\lambda c_{\lambda\theta}^2 - s_{\lambda\theta}s_\lambda c_{\lambda\theta}sh_\lambda + c_\lambda sh_\lambda \\ &= 0. \end{aligned} \tag{12}$$

Here $s_{(\bullet)}=\sin(\bullet)$, $sh_{(\bullet)}=\sinh(\bullet)$, $c_{(\bullet)}=\cos(\bullet)$, and $ch_{(\bullet)}=\cosh(\bullet)$. If the added mass is zero, then substituting $\Delta M=0$ and $\theta=0$ one can see that Eq. (12) reduces to Eq. (9).

III. THE GENERAL DERIVATION OF CALIBRATION CONSTANTS

The equations in the previous section are obtained by considering the differential equation and the boundary conditions in an exact manner. These equations are complex enough so that a simple relationship between the change in the mass and the shift in frequency is not available. Moreover, these equations are valid for point mass only. Many biological objects are relatively large in dimension and, therefore, the assumption that the mass is concentrated at one point may not be valid. In this section we develop a new approach to address these problems.

In the fundamental mode of vibration, the natural frequency of a SWCNT oscillator can be expressed as

$$fn=\frac{1}{2\pi}\sqrt{\frac{k_{eq}}{m_{eq}}}. \tag{13}$$

Here k_{eq} and m_{eq} are, respectively, equivalent stiffness and mass of SWCNT in the first mode of vibration. The equivalent mass m_{eq} changes depending on whether a nano-object is attached to the CNT. This in turn changes the natural frequency. Here we use an energy based approach to obtain k_{eq} and m_{eq}. Suppose Y_j is the assumed displacement function for the first mode of vibration. Depending on the boundary conditions, it can be given by either Eq. (4) or Eq. (10). Suppose the added mass occupies a length γL and its mass per unit length is m [see Figs. 1(b) and 1(d) and Figs. 2(b) and 2(d)] Therefore, $M=m\times\gamma L$. From the kinetic energy of the SWCNT with the added mass and assuming harmonic motion, the overall equivalent mass m_{eq} can be expressed as

$$m_{eq}=\rho AL\underbrace{\int_0^1 Y_j^2(\xi)d\xi}_{I_1}+M\underbrace{\int_\Gamma Y_j^2(\xi)d\xi}_{I_2}, \tag{14}$$

where Γ is the domain of the additional mass. From the

potential energy, the equivalent stiffness k_{eq} can be obtained as

$$k_{eq} = \frac{EI}{L^3} \underbrace{\int_0^1 Y_j''^2(\xi) \mathrm{d}\xi}_{I_3}. \tag{15}$$

From these expressions we have

$$\frac{k_{eq}}{m_{eq}} = \frac{EI/L^3 I_3}{\rho A L I_1 + M I_2} = \left(\frac{EI}{\rho A L^4}\right) \frac{I_3}{I_1 + I_2 \Delta M}, \tag{16}$$

where the mass ratio ΔM is defined in Eq. (8). Using the expression of the natural frequency we have

$$f_n = \frac{1}{2\pi} \sqrt{\frac{k_{eq}}{m_{eq}}} = \frac{\beta}{2\pi} \frac{c_k}{\sqrt{1 + c_m \Delta M}}, \tag{17}$$

where

$$\beta = \sqrt{\frac{EI}{\rho A L^4}}, \tag{18}$$

the stiffness calibration constant

$$c_k = \sqrt{\frac{I_3}{I_1}}, \tag{19}$$

and the mass calibration constant

$$c_m = \frac{I_2}{I_1}. \tag{20}$$

Equation (17), together with the calibration constants gives an explicit relationship between the change in the mass and frequency.

Clearly the resonant frequency of a SWCNT with no added mass is obtained by substituting $\Delta M = 0$ in Eq. (17) as

$$f_{0_n} = \frac{1}{2\pi} c_k \beta \tag{21}$$

Combining Eqs. (17) and (21) one obtains the relationship between the resonant frequencies as

$$f_n = \frac{f_{0_n}}{\sqrt{1 + c_m \Delta M}}. \tag{22}$$

The frequency shift can be expressed using Eq. (22) as

$$\Delta f = f_{0_n} - f_n = f_{0_n} - \frac{f_{0_n}}{\sqrt{1 + c_m \Delta M}}. \tag{23}$$

From this we obtain

$$\frac{\Delta f}{f_{0_n}} = 1 - \frac{1}{\sqrt{1 + c_m \Delta M}}. \tag{24}$$

Rearranging gives the expression

$$\Delta M = \frac{1}{c_m \left(1 - \frac{\Delta f}{f_{0_n}}\right)^2} - \frac{1}{c_m}. \tag{25}$$

This equation completely relates the change in mass with the frequency shift using the mass calibration constant. The actual value of the added mass can be obtained from (25) as

$$M = \frac{\rho A L}{c_m} \frac{(c_k^2 \beta^2)}{(c_k \beta - 2\pi \Delta f)^2} - \frac{\rho A L}{c_m} \tag{26}$$

This is the general equation which completely relates the added mass and the frequency shift using the calibration constants. These calibration constants change depending on the boundary conditions and geometry of the added mass. Next, we calculate their values.

IV. CALCULATION OF THE CALIBRATION CONSTANTS

We fist consider the cantilevered CNT with an added point mass. For the cantilevered CNT, we use the mode shape in (4) as the assumed deflection shape Y_j. The value of λ_j appearing in this equation is 1.8751. Using these, the integral I_1 can be obtained as

$$I_1 = \int_0^1 Y_j^2(\xi) \mathrm{d}\xi = 1.0. \tag{27}$$

For the point mass at the end of the cantilevered SWNT we have

$$m(\xi) = M \delta(\xi - 1). \tag{28}$$

Using these, the integral I_2 can be obtained as

$$I_2 = \int_0^1 \delta(\xi - 1) Y_j^2(\xi) \mathrm{d}\xi = Y_j^2(1) = 4.0. \tag{29}$$

Differentiating $Y_j(\xi)$ in Eq. (4) with respect to ξ twice, we obtain

$$I_3 = \int_0^1 Y_j''^2(\xi) \mathrm{d}\xi = 12.3624. \tag{30}$$

Using these integrals, the stiffness and mass calibration factors can be obtained as

$$c_k = \sqrt{\frac{I_3}{I_1}} = 3.5160 \quad \text{and} \quad c_m = \frac{I_2}{I_1} = 4.0. \tag{31}$$

Now we consider the case when the mass is distributed over a length γL from the edge of the cantilevered CNT. Since the total mass is M, the mass per unit length is $M/\gamma L$. Noting that the added mass is between $(1-\gamma)L$ to L, the integral I_2 can be expressed as

$$I_2 = \frac{1}{\gamma} \int_{\xi=1-\gamma}^1 Y_j^2(\xi) \mathrm{d}\xi; \quad 0 \le \gamma \le 1. \tag{32}$$

This integral can be calculated for different values of γ.

The same approach can be used for the bridged CNT also. In this case Y_j given by Eq. (10) need to be used. The

TABLE I. The stiffness (c_k) and mass (c_m) calibration constants for CNT based bionanosensor. The value of γ indicates the length of the mass as a fraction of the length of the CNT.

	Cantilevered CNT		Bridged CNT	
Mass size	c_k	c_m	c_k	c_m
Point mass ($\gamma \to 0$)	3.516 0152	4.0	22.373 285	2.522 208 547
$\gamma=0.1$		3.474 732 666		2.486 573 805
$\gamma=0.2$		3.000 820 053		2.383 894 805
$\gamma=0.3$		2.579 653 837		2.226 110 255
$\gamma=0.4$		2.212 267 400		2.030 797 235
$\gamma=0.5$		1.898 480 438		1.818 142 650
$\gamma=0.6$		1.636 330 135		1.607 531183
$\gamma=0.7$		1.421 839 146		1.414 412512
$\gamma=0.8$		1.249 156 270		1.248 100151

integrals can be obtained in a manner similar to that of the cantilevered case. For the bridged CNT with a point mass at the center, we have

$$I_2 = \int_0^1 \delta(\xi - 1/2) Y_j^2(\xi) \mathrm{d}\xi = Y_j^2(1/2) = 2.5222. \tag{33}$$

For the case of distributed added mass of length γ placed symmetrically about the center, the mass occupies a space between $x=(1-\gamma)L/2$ to $x=(1+\gamma)L/2$ as seen in Fig. 2(d). Therefore, we have

$$I_2 = \frac{1}{\gamma} \int_{\xi=(1-\gamma)/2}^{\xi=(1+\gamma)/2} Y_j^2(\xi) \mathrm{d}\xi; \quad 0 \le \gamma \le 1. \tag{34}$$

The values of the calibration constants for different selected values of γ are shown in Table I. It can be seen that with the increase in the value of γ, the value of the mass calibration constant decreases. Therefore, according to Eq. (23), this in turn will make the sensor less sensitive.

V. VIBRATIONAL ANALYSIS OF CNTS USING MOLECULAR MECHANICS APPROACH

In the calculation, GAUSSIAN 09 computer software[44] and the UFF developed by Rappe *et al.*[36] are employed. The UFF is a harmonic force field, in which the general expression of total energy is a sum of energies due to valence or bonded interactions and nonbonded interactions

$$E = \sum E_R + \sum E_\theta + \sum E_\phi + \sum E_\omega + \sum E_{\mathrm{VDW}} + \sum E_{el}. \tag{35}$$

The valence interactions consist of bond stretching (E_R) and angular distortions. The angular distortions are bond angle bending (E_θ), dihedral angle torsion (E_ϕ) and inversion terms (E_ω). The nonbonded interactions consist of van der Waals (E_{VDW}) and electrostatic (E_{el}) terms. In this study, we used UFF model,[36] wherein the force field parameters are estimated using general rules based only on the element, its hybridization and its connectivity. The force field functional forms and parameters used in this study are in accordance with.[36] The functional form of above energy terms is given as follows:

$$E_R = k_1(r - r_0)^2$$

$$E_\theta = k_2(C_0 + C_1 \cos\theta + C_2 \cos 2\theta)$$

$$C_2 = \frac{1}{4 \sin^2 \theta}$$

$$C_1 = -4C_2 \cos\theta_0$$

$$C_0 = C_2(2\cos^2\theta_0 + 1)$$

$$E_\phi = k_3(1 \pm \cos n\phi)$$

$$E_\omega = k_4[1 \pm \cos(n\chi - \chi_0)]$$

$$E_{\mathrm{vdW}} = D\left[\left(\frac{r^*}{r}\right)^{12} - 2\left(\frac{r^*}{r}\right)^6\right]$$

$$\text{and } E_{el} = \frac{q_i q_j}{\varepsilon r_{ij}} \tag{36}$$

Here k_1, k_2, k_3, and k_4 are force constants, θ_0 is the natural bond angle, D is the van der Waals well depth, r^* is the van der Waals length, q_i is the net charge of an atom, ε is the dielectric constant, and r_{ij} is the distance between two atoms. In the calculation, the difference of nonpolar and polar semiconductors is dependent of the net charge q_i being set to zero or not. Detailed values of these parameters in Eq. (36) can be found in Ref. 36 and the frequency calculation can be found in Ref. 45. In order to verify the accuracy of the methodology adopted, we validated our computed frequencies of SWCNT resonators with molecular dynamics (MD) simulation results presented in Ref. 46. First four natural frequencies of a (5,5) CNT for different values of the aspect ratio is considered. Our results are tabulated in Table II, which are in good agreement with previous studies. More detailed study using present approach is illustrated in Ref. 45. This comparison provides the confidence for the use of this model in further investigations as a mass sensor.

VI. RESULTS AND DISCUSSIONS

From the developments in Secs. II and III two methods to identify the added mass from the frequency shift emerges. The first approach uses the exact solution of the transcendental frequency equation and the second approach uses the closed-form expressions involving the calibration constants. The first approach is exact but do not result in any simple sensor equation. The relative frequency shift can be obtained as

$$\frac{\Delta f}{f_{0_n}} = \frac{\lambda_{0_1}^2 - \lambda_1^2}{\lambda_{0_1}^2}. \tag{37}$$

Here the values of λ_{0_1} correspond to the CNT without the added mass. For the cantilevered and the bridged case, λ_{0_1} is, respectively, 1.8751 and 4.7300. The values of λ_1 correspond

TABLE II. Natural frequencies of a (5,5) CNT in THz—cantilever boundary condition. First four natural frequencies obtained from the present approach is compared with the MD simulation[46] for different values of the aspect ratio.

	Present analysis				MD simulation[a]			
Aspect ratio	1st	2nd	3rd	4th	1st	2nd	3rd	4th
5.26	0.220	1.113	2.546	4.075	0.212	1.043	2.340	3.682
5.62	0.195	1.005	2.325	3.759	0.188	0.943	2.141	3.406
5.99	0.174	0.912	2.132	3.478	0.167	0.857	1.967	3.158
6.35	0.156	0.830	1.961	3.226	0.150	0.782	1.813	2.936
6.71	0.141	0.759	1.810	3.000	0.136	0.716	1.676	2.736
7.07	0.128	0.696	1.675	2.797	0.123	0.657	1.553	2.555
7.44	0.116	0.641	1.554	2.614	0.112	0.605	1.443	2.392
7.80	0.106	0.592	1.446	2.447	0.102	0.559	1.344	2.243
8.16	0.098	0.548	1.348	2.296	0.094	0.518	1.255	2.108
8.52	0.089	0.492	1.231	2.102	0.086	0.481	1.174	1.984

[a]Reference 46.

to the mass loaded CNT and should be obtained by solving Eqs. (7) and (12) for the cantilevered and the bridged case, respectively.

In Fig. 3 the identified mass from the frequency shift in a cantilevered CNT is shown. We use a zigzag (5,0) SWCNT of length 8.52 nm and the added mass is assumed to be deoxythymidine, a nucleotide that is found in DNA. The added mass and the corresponding frequency shift are calculated from the molecular mechanics approach explained in Sec. V. These frequency shifts are considered as "experimental results" and used in the sensor Eq. (25). The value of the mass predicted by this equation are then compared with the known values used in the molecular mechanics simulations. The calibration constant based approach is verified with the exact approach in Fig. 3(a) for the case of point mass. It can be seen that the results from the simple calibration constant based approach match the exact results obtained by solving the transcendental Eq. (7). By comparing the identified mass with the molecular mechanics simulations in Fig. 3(a), we can see that the sensor Eq. (25) slightly over-predicts the mass. The general trend is, however, similar. Percentage error obtained using the proposed method is shown in Table III. The error is calculated with respect to the molecular mechanics simulation results. From the table one can see that the maximum error in the identified mass is about 34%. No particular pattern with respect to the frequency shift is observed.

The case of distributed mass is considered in Fig. 3(b). For the results shown here the value of γ varies between 0.05 to 0.72. Equation (25) with the γ-dependent mass calibration constant gives excellent agreement with the molecular mechanics simulations. Percentage error obtained using the proposed method is shown in Table III for different values of frequency shift and γ. One can observe that the maximum error in the identified mass is about 14%. No particular pattern of the error with respect to the frequency shift or γ is observed. The values, one would obtain using the point mass assumption, is also shown in Fig. 3(b). The importance of using the calibration constant varying with the length of the mass is clear from this comparative study. A point mass

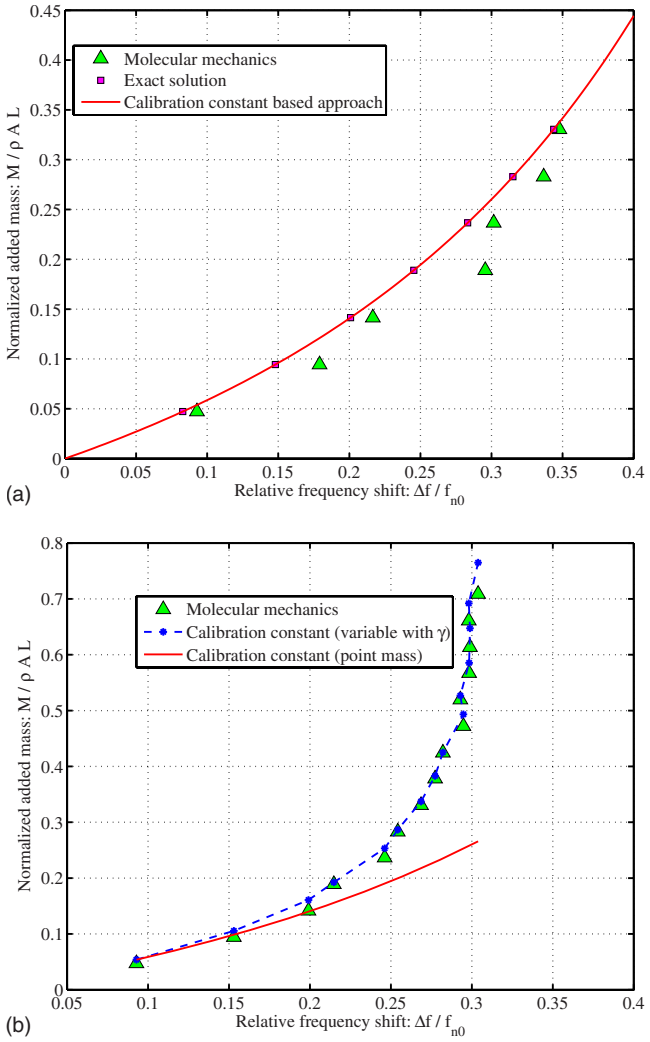

FIG. 3. (Color online) Identified attached masses from the frequency shift in a cantilevered CNT. The proposed calibration constant based approach is validated using data from the molecular mechanics simulations. The importance of using the calibration constant varying with the length of the mass can be seen in (b). The point mass assumption often used in cantilevered sensors, can result in significant error when the mass is distributed in nature.

TABLE III. Percentage error in the mass detection using cantilevered CNT based bionanosensor. The average errors for the point and distributed mass cases are, respectively, 16.1520% and 5.3581%.

Point mass		Distributed mass		
Relative frequency shift ($\Delta f/f_{0_n}$)	Percentage error	Relative frequency shift ($\Delta f/f_{0_n}$)	Normalized length (γ)	Percentage error
0.0929	13.9879	0.0929	0	13.9879
0.1790	28.1027	0.1530	0.0500	11.8626
0.2165	11.1765	0.1991	0.1000	13.7038
0.2956	34.2823	0.2148	0.1500	1.7865
0.3016	10.9296	0.2462	0.2000	7.0172
0.3367	12.4422	0.2542	0.2500	1.3278
0.3477	2.1427	0.2687	0.3000	1.9943
		0.2773	0.3500	1.2631
		0.2821	0.4000	0.1653
		0.2948	0.4500	4.5150
		0.2929	0.5000	1.3776
		0.2983	0.5500	3.2275
		0.2989	0.6167	5.5240
		0.2981	0.6667	4.6735
		0.3039	0.7167	7.9455

assumption, often used in cantilevered CNT sensors, can result in significant error when the mass is distributed in nature.

In Fig. 4 the identified mass from the frequency shift in a bridged CNT is shown. The added mass and the corresponding frequency shift are calculated from the molecular mechanics approach. The calibration constant based approach is verified with the exact approach in Fig. 4(a) for the case of point mass. It can be seen that, like the cantilevered case, the results from the simple calibration constant based approach match the exact results obtained by solving the transcendental Eq. (12). By comparing the identified mass with the molecular mechanics simulations in Fig. 4(a), we can see that the sensor Eq. (25) predicts the added mass very accurately. The case of distributed mass is considered in Fig. 4(b). The value of γ varies between 0.1 to 0.6. Equation (25) with the γ-dependent mass calibration constant gives good agreement with the molecular mechanics simulations. The values, one would obtain using the point mass assumption, is also shown in Fig. 4(b). The distributed nature of the mass clearly has an effect, but it is less prominent compared to the cantilevered sensor. Percentage error obtained using the proposed method is shown in Table IV for both point and distributed mass. One can observe that the maximum error in the identified mass is about 12% for the point mass case and 23% for the distributed mass case. The error for the distributed mass case shows an increasing trend with the increase in the value of γ. However, for the point mass case, no particular pattern of the error with respect to the frequency shift is observed.

VII. CONCLUSIONS

The possibility of using SWCNT as a nanoscale mass sensor is investigated using the shift in the resonance frequencies. The SWCNT resonators are assumed to be either in cantilevered or in bridged configurations. For each configurations, two types of mass loadings, namely, point mass and

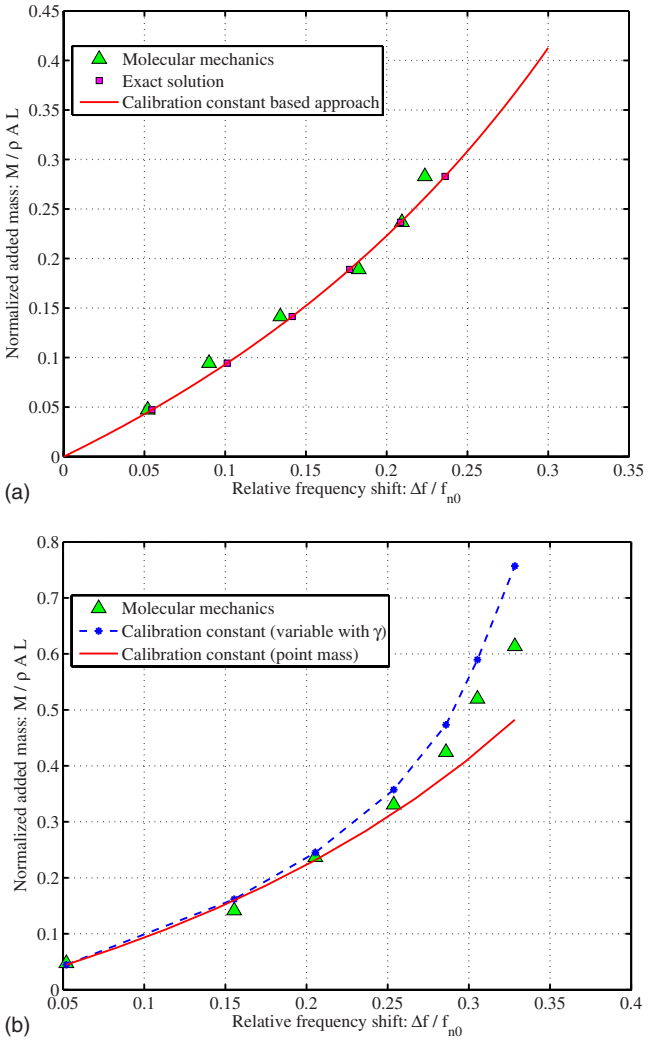

FIG. 4. (Color online) Identified attached masses from the frequency shift in a bridged CNT. The proposed calibration constant based approach is validated using data from the molecular mechanics simulations. Again, the importance of using the calibration constant varying with the length of the mass can be seen in (b). However, the difference between the point mass and distributed mass assumption is not as significant as the cantilevered case.

TABLE IV. Percentage error in the mass detection using bridged CNT based bionanosensor. The average errors for the point and distributed mass cases are, respectively, 6.1226% and 11.3554%.

Point mass		Distributed mass		
Relative frequency shift ($\Delta f/f_{0_n}$)	Percentage error	Relative frequency shift ($\Delta f/f_{0_n}$)	Normalized length (γ)	Percentage error
0.0521	5.1632	0.0521	0	5.1636
0.0901	12.7402	0.1555	0.1000	14.2792
0.1342	6.4153	0.2055	0.2000	3.5290
0.1827	4.2630	0.2538	0.3000	8.1455
0.2094	0.5273	0.2859	0.4000	11.5109
0.2237	7.6267	0.3053	0.5000	13.4830
		0.3284	0.6000	23.3768

distributed mass, have been considered. For the case of point mass, closed-form transcendental equations have been derived for the resonance frequencies for both types of configurations using the Euler–Bernoulli beam theory. Since these equations do not result a simple relationship between the frequency shift and the added mass, an energy based method is proposed. Using this, generalized calibration constants have been derived for an explicit relationship between the added mass and the frequency shift. Integral expressions of the calibration constants have been given and their values have been obtained for the case of point mass and distributed mass with both type of configurations. A molecular mechanics based approach is used to validate the calibration constant based sensor equations. We used the UFF model, wherein, the force field parameters are estimated using the general rules based on the element, its hybridization and its connectivity. Acceptable agreements between the proposed approach and the molecular mechanics simulations have been observed (the average error varies approximately between 5%–15% for the examples considered). Our results indicate that the distributed nature of the mass has considerable influence on the performance of the sensor. The cantilevered SWCNT sensor turned out to be more sensitive with respect to the mass distribution compared to the bridged SWCNT sensor. As a result, for the cantilevered SWCNT sensor, the point mass assumption may lead to significant error when the true mass is distributed in nature. The present method is expected to give accurate results if the location and distribution of the added mass are known. Further research is necessary, when in addition to the total mass, these quantities are also need to be identified simultaneously.

ACKNOWLEDGMENTS

S.A. gratefully acknowledges the support of The Leverhulme Trust for the award of the Philip Leverhulme Prize. R.C. acknowledges the support of Royal Society through the award of Newton International Fellowship.

[1] S. V. Rotkin and S. Subramoney, *Applied Physics of Carbon Nanotubes: Fundamentals of Theory, Optics, and Transport Devices* (Springer-Verlag, Berlin, Heidelberg, 2005).
[2] Y. Yun, Z. Dong, V. Shanov, W. R. Heineman, H. B. Halsall, A. Bhattacharya, L. Conforti, R. K. Narayan, W. S. Ball, and M. J. Schulz, Nanotoday **2**, 30 (2007).
[3] G. A. Rivas, M. D. Rubianes, M. C. Rodriguez, N. E. Ferreyra, G. L. Luque, M. L. Pedano, S. A. Miscoria, and C. Parrado, Talanta **74**, 291 (2007).
[4] A. Fennimore, T. Yuzvinsky, W. Han, M. Fuhrer, J. Cumings, and A. Zettl, Nature (London) **424**, 408 (2003).
[5] J. Wang, Electroanalysis **17**, 7 (2005).
[6] O. Kumar, Y. Singh, V. K. Rao, and R. Vijayaraghavan, Def. Sci. J. **58**, 617 (2008).
[7] J.-W. Kang and H.-J. Hwang, J. Comput. Theor. Nanosci. **6**, 2347 (2009).
[8] N. W. S. Kam, M. O'Connell, J. A. Wisdom, and H. Dai, Proc. Natl. Acad. Sci. U.S.A. **102**, 11600 (2005).
[9] L. Lacerda, S. Raffa, M. Prato, A. Bianco, and K. Kostarelos, Nanotoday **2**, 38 (2007).
[10] M. Prato, K. Kostarelos, and A. Bianco, Acc. Chem. Res. **41**, 60 (2008).
[11] H. Wang, L. Gu, Y. Lin, F. Lu, M. J. Meziani, P. G. Luo, W. Wang, L. Cao, and Y.-P. Sun, J. Am. Chem. Soc. **128**, 13364 (2006).
[12] K. Jensen, K. Kim, and A. Zettl, Nat. Nanotechnol. **3**, 533 (2008).
[13] E. Gil-Santos, D. Ramos, A. Jana, M. Calleja, A. Raman, and J. Tamayo, Nano Lett. **9**, 4122 (2009).
[14] Y. Li, X. Qiu, F. Yang, X.-S. Wang, and Y. Yin, Nanotechnology **19**, 225701 (2008).
[15] S. K. Georgantzinos and N. K. Anifantis, Physica E **42**, 1795 (2010).
[16] K. R. Byun, K. Lee, and O. K. Kwon, J. Comput. Theor. Nanosci. **6**, 2393 (2009).
[17] R. Chowdhury, S. Adhikari, and J. Mitchell, Physica E **42**, 104 (2009).
[18] B. L. Allen, P. D. Kichambare, and A. Star, Adv. Mater. **19**, 1439 (2007).
[19] K. Balasubramanian and M. Burghard, Anal. Bioanal. Chem. **385**, 452 (2006).
[20] S. B. Tooski, J. Appl. Phys. **107**, 014702 (2010).
[21] J. Wang and M. Musameh, Anal. Chem. **75**, 2075 (2003).
[22] S. Tsang, J. Davis, M. Green, H. Allen, O. Hill, Y. Leung, and P. Sadler, J. Chem. Soc., Chem. Commun. **1995**, 1803 (1995).
[23] J. Davis, M. Green, H. Hill, Y. Leung, P. Sadler, J. Sloan, A. Xavier, and S. Tsang, Inorg. Chim. Acta **272**, 261 (1998).
[24] S. S. Wong, E. Joselevich, A. T. Woolley, C. L. Cheung, and C. M. Lieber, Nature (London) **394**, 52 (1998).
[25] R. Baughman, C. Cui, A. Zakhidov, Z. Iqbal, J. Barisci, G. Spinks, G. Wallace, A. Mazzoldi, D. De Rossi, A. Rinzler, O. Jaschinski, S. Roth, and M. Kertesz, Science **284**, 1340 (1999).
[26] M. Mattson, R. Haddon, and A. Rao, J. Mol. Neurosci. **14**, 175 (2000).
[27] F. Lu, L. Gu, M. J. Meziani, X. Wang, P. G. Luo, L. M. Veca, L. Cao, and Y.-P. Sun, Adv. Mater. **21**, 139 (2009).
[28] D. Du, M. Wang, J. Cai, Y. Qin, and A. Zhang, Sens. Actuators B **143**, 524 (2010).
[29] J. Davis, K. Coleman, B. Azamian, C. Bagshaw, and M. Green, Chem.-Eur. J. **9**, 3732 (2003).
[30] S. Lee and D. S. Yoon, BioChip J. **1**, 193 (2007).
[31] R. Chen, S. Bangsaruntip, K. Drouvalakis, N. Kam, M. Shim, Y. Li, W. Kim, P. Utz, and H. Dai, Proc. Natl. Acad. Sci. U.S.A. **100**, 4984 (2003).
[32] J. Gooding, R. Wibowo, J. Liu, W. Yang, D. Losic, S. Orbons, F. Mearns, J. Shapter, and D. Hibbert, J. Am. Chem. Soc. **125**, 9006 (2003).
[33] J. Li, H. Ng, A. Cassell, W. Fan, H. Chen, Q. Ye, J. Koehne, J. Han, and M. Meyyappan, Nano Lett. **3**, 597 (2003).
[34] L.-C. Jiang and W.-D. Zhang, Biosens. Bioelectron. **25**, 1402 (2010).
[35] C. Y. Li and T. W. Chou, Appl. Phys. Lett. **84**, 5246 (2004).
[36] A. K. Rappe, C. J. Casewit, K. S. Colwell, W. A. Goddard, and W. M. Skiff, J. Am. Chem. Soc. **114**, 10024 (1992).
[37] C. Y. Wang, C. Q. Ru, and A. Mioduchowski, J. Nanosci. Nanotechnol. **3**, 199 (2003).
[38] F. Scarpa and S. Adhikari, J. Non-Cryst. Solids **354**, 4151 (2008).
[39] C. Y. Wang, C. Q. Ru, and A. Mioduchowski, Phys. Rev. B **72**, 075414 (2005).
[40] F. Scarpa and S. Adhikari, J. Phys. D **41**, 085306 (2008).
[41] R. Chowdhury, C. Y. Wang, and S. Adhikari, J. Phys. D **43**, 085405 (2010).
[42] D. Wu, W. Chien, C. Chen, and H. Chen, Sens. Actuators, A **126**, 117 (2006).
[43] R. D. Blevins, *Formulas for Natural Frequency and Mode Shape* (Krieger, Malabar, Florida, 1984).
[44] M. J. Frisch, G. W. Trucks, H. B. Schlegel, G. E. Scuseria, M. A. Robb, J. R. Cheeseman, G. Scalmani, V. Barone, B. Mennucci, G. A. Petersson *et al.*, GAUSSIAN 09 Revision A.1.
[45] R. Chowdhury, S. Adhikari, C. Y. Wang, and F. Scarpa, Comput. Mater. Sci. **48**, 730 (2010).
[46] W. H. Duan, C. M. Wang, and Y. Y. Zhang, J. Appl. Phys. **101**, 024305 (2007).